

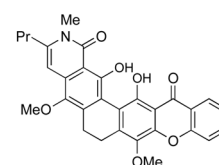
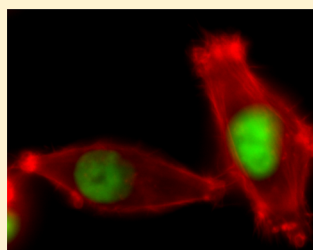
# Synthesis and Biological Evaluation of Kibdelone C and Its Simplified Derivatives

Janjira Rujirawanich,<sup>†</sup> Soyeon Kim,<sup>‡</sup> Ai-Jun Ma,<sup>†</sup> John R. Butler,<sup>†</sup> Yizhong Wang,<sup>†</sup> Chao Wang,<sup>†</sup> Michael Rosen,<sup>‡</sup> Bruce Posner,<sup>†</sup> Deepak Nijhawan,<sup>c,†</sup> and Joseph M. Ready<sup>\*,†</sup>

<sup>†</sup>Department of Biochemistry and <sup>‡</sup>Department of Internal Medicine, UT Southwestern Medical Center, 5323 Harry Hines Boulevard, Dallas, Texas 75390-9038, United States

**S** Supporting Information

**ABSTRACT:** Polycyclic tetrahydroxanthones comprise a large class of cytotoxic natural products. No mechanism of action has been described for any member of the family. We report the synthesis of kibdelone C and several simplified analogs. Both enantiomers of kibdelone C show low nanomolar cytotoxicity toward multiple human cancer cell lines. Moreover, several simplified derivatives with improved chemical stability display higher activity than the natural product itself. In vitro studies rule out interaction with DNA or inhibition of topoisomerase, both of which are common modes of action for polycyclic aromatic compounds. However, cellular studies reveal that kibdelone C and its simplified derivatives disrupt the actin cytoskeleton without directly binding actin or affecting its polymerization in vitro.



Simplified derivative of kibdelone C

## INTRODUCTION

Kibdelones A–C (Scheme 1, 1–3) are members of a growing class of natural products characterized by a hexacyclic, polyaromatic scaffold and a tetrahydroxanthone moiety.<sup>1,2</sup> These microbial metabolites arise biosynthetically from multiple cyclizations from a single polyacetate chain, accounting for the high degree of oxygenation on the aromatic and heteroaromatic rings.<sup>3</sup> Structurally related natural products include simaomicin  $\alpha$ ,<sup>4</sup> actinoplanone,<sup>5</sup> SCH-56036,<sup>6</sup> and kigamicin A.<sup>7</sup> Additionally, natural products such as cervinomycin A2<sup>8</sup> and FD-594<sup>9</sup> feature aromatic F-rings as part of a xanthone moiety. All of these secondary metabolites share a common hexacyclic core structure and differ with regard to the substitution pattern on the aryl and heteroaryl rings. They display potent cytotoxicity, although no mechanism of action has been elucidated for any member of the family. In particular, they generally show broad-spectrum toxicity, including anticancer, antibiotic, and antifungal activity. Simaomicin  $\alpha$  has shown activity preventing coccidiosis in chickens<sup>4b</sup> and was found to induce G1 arrest in cultured cancer cells.<sup>4c</sup> Likewise, the kigamicins have demonstrated efficacy in inhibiting tumor growth in immunocompromised mice.<sup>7c</sup> Despite these promising biological activities, little is understood regarding the mechanism by which polycyclic tetrahydroxanthone natural products kill microbial and mammalian cells.

The Capon group discovered the kibdelones in the culture media of a soil actinomycete *Kibdelosporangium* sp.<sup>1,10</sup> Extensive one- and two-dimensional NMR data revealed the presence of a chlorinated isoquinolinone AB ring system. The DEF-ring tetrahydroxanthone included three stereogenic hydroxyl groups with the relative stereochemistry shown in

Scheme 1. The three congeners vary in the oxidation state of the B ring (quinone vs hydroquinone) and the C ring (saturated vs unsaturated). Furthermore, their isolation revealed that kibdelone C could spontaneously oxidize to kibdelones A and B under aerobic conditions.

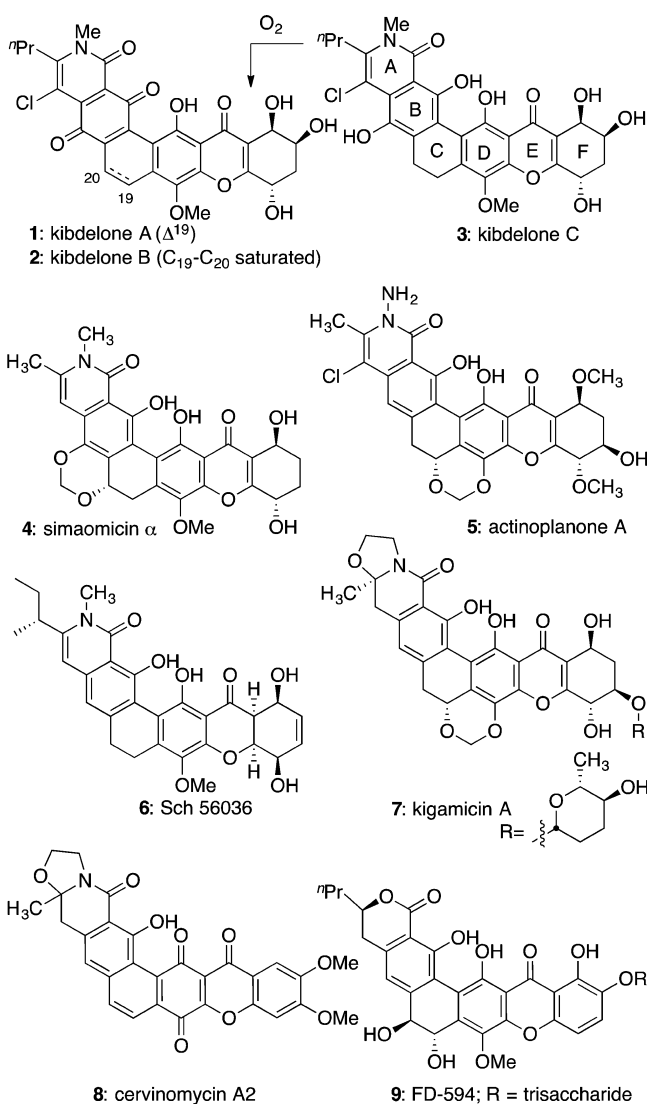
The kibdelones displayed potent cytotoxicity against a panel of human cancer cell lines. All three compounds arrested growth of cell lines derived from lung, colon, ovarian, prostate, breast, and other tumor types with GI<sub>50</sub> values <5 nM. They additionally showed robust toxicity toward *Bacillus subtilis* bacteria. It is unclear if the kibdelones A–C are in fact equally active or if they interconvert under the conditions of the biological assays. The NCI COMPARE analysis did not reveal a strong correlation between the toxicity profile of the kibdelones and that of other known cytotoxins, indicating that they might operate through a novel mode of action.

The combination of unique structural features and compelling biological properties make the polycyclic xanthone natural products attractive targets for total synthesis.<sup>2</sup> The Kelly group described the first synthesis of the xanthone-containing natural products cervinomycins A1 and A2,<sup>11</sup> and reports from the Rao and Mehta groups followed shortly thereafter.<sup>12,13</sup> The Suzuki group made an important contribution to the area with a synthesis of FD-594 aglycon; theirs was the first enantioselective synthesis of a member of the family.<sup>14</sup> The Porco group reported an elegant synthesis of the naturally occurring (+)-kibdelone C,<sup>15</sup> and we described a synthesis of (–)-simaomicin  $\alpha$  in 2013.<sup>16</sup> More recently, the Martin group

Received: May 27, 2016

Published: July 26, 2016

## Scheme 1. Hexacyclic Tetrahydroxanthone and Xanthone Natural Products



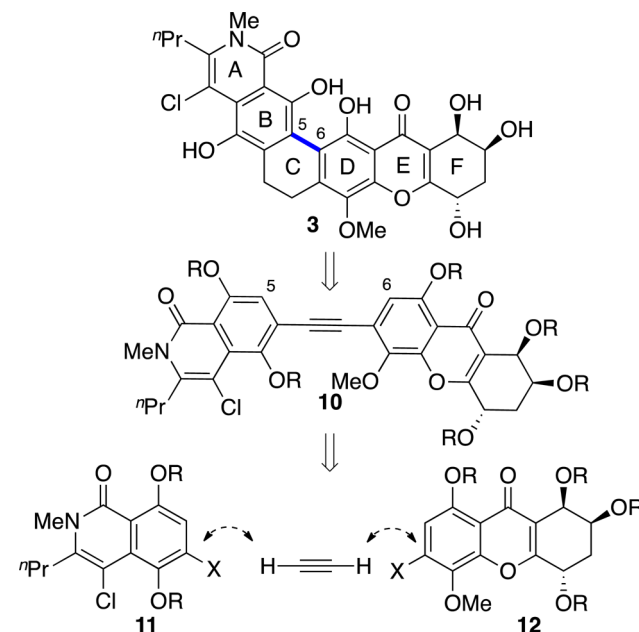
described a total synthesis of the aglycon of IB-00208.<sup>17</sup> Additionally, several groups have reported synthetic studies toward natural products of the hexacyclic xanthone family.<sup>18</sup>

We set as an initial objective the development of a flexible and enantioselective synthetic route that could provide access to the natural product and allow assignment of the absolute stereochemistry of 1–3.<sup>19</sup> On the basis of initial biological results described below, we then pursued simplified analogues of the kibdelones. Here we describe the evolution of our synthetic strategy, the synthesis of simplified analogues maintaining full biological activity, and initial efforts to understand the mode of action of the kibdelones.

## RESULTS AND DISCUSSION

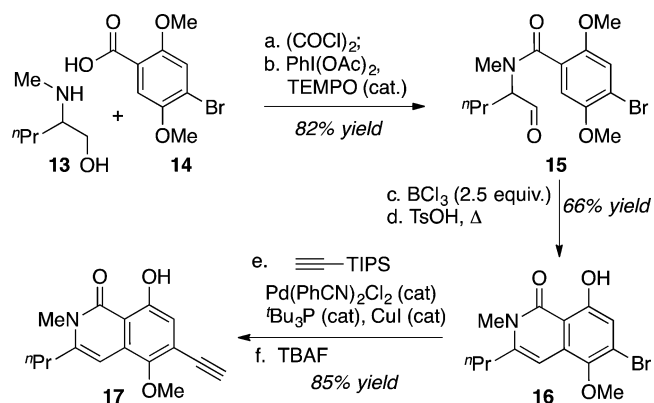
**Synthetic Strategy.** In considering a synthetic approach to the kibdelones and related natural products, we targeted the C5–C6 bond that connects the B- and D-rings (Scheme 2). Strategically, retrosynthetic disconnection of this bond would deconstruct the C-ring to suggest an intermediate such as diaryl alkyne 10, in which the isoquinoline and tetrahydroxanthone moieties can be viewed as independent ring systems. From a tactical perspective, we were attracted to a late-stage C5–C6

## Scheme 2. Synthetic Strategy



bond construction, because multiple methods exist for the formation of biaryl bonds, including cross-coupling, oxidative coupling, and C–H functionalization reactions. Finally, we reasoned that the isoquinolinone fragment 11 could be joined to tetrahydroxanthone subunit 12 using an equivalent of acetylene as a lynchpin.

**Fragment Synthesis.** To prepare the isoquinolinone AB-rings, we explored cyclization of aryl aldehyde 15 (Scheme 3).

Scheme 3. Synthesis of the AB-Ring Isoquinolinone<sup>a</sup>

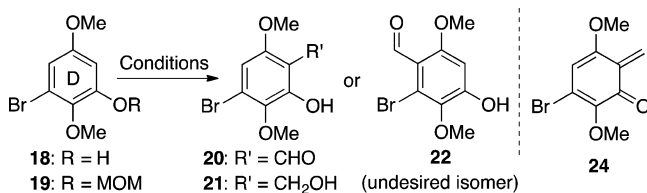
<sup>a</sup>(a)  $(\text{COCl})_2$ , DMF (cat),  $\text{CH}_2\text{Cl}_2$ ;  $\text{CH}_2\text{Cl}_2/5 \text{ M NaOH } 1.5:1$ . (b)  $\text{PhI(OAc)}_2$ , TEMPO (10 mol %),  $\text{CH}_2\text{Cl}_2$ , 82% yield over two steps. (c)  $\text{BCl}_3$  (1.0 equiv, then 1.5 equiv), 0 °C to rt. (d)  $\text{TsOH}\cdot\text{H}_2\text{O}$  (1.5 equiv), toluene, reflux, 66% yield over two steps. (e)  $\text{Pd(PhCN)}_2\text{Cl}_2$  (5 mol %),  $\text{'Bu}_3\text{P}\cdot\text{HBF}_4$  (10 mol %),  $\text{CuI}$  (3 mol %),  $\text{Et}_2\text{NH}$ , 40 °C. (f)  $\text{Bu}_4\text{NF}$  (1.5 equiv), 85% yield over two steps.

To this end, amino alcohol 13<sup>20</sup> was coupled to the acid chloride derived from benzoic acid 14.<sup>21</sup> Subsequent oxidation generated the cyclization substrate, aldehyde 15. Both  $\text{BCl}_3$  and  $\text{BBr}_3$  promoted electrophilic addition to yield a benzylic alcohol (not shown), which could be dehydrated to yield isoquinolinone 16 under acidic conditions. While  $\text{BCl}_3$  only demethylated the phenol ortho to the amide,  $\text{BBr}_3$  yielded a doubly demethylated material. It is unclear if demethylation is required

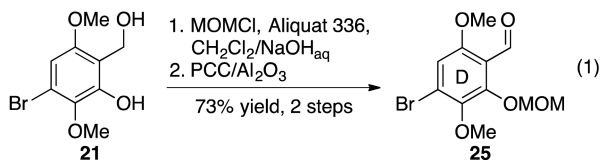
for cyclization, but we note that we never observed cyclized products that retained both methyl groups. Moreover, the highest yields were obtained when the  $\text{BCl}_3$  was added in two portions, 1 equiv followed by 1.5 equiv. Monitoring of a reaction in  $\text{CDCl}_3$  by  $^1\text{H}$  NMR revealed that the first equivalent of  $\text{BCl}_3$  completely consumed aldehyde **15** to form an intermediate we characterized as a chlorohydrin.<sup>22</sup> Subsequent addition of the remaining 1.5 equiv of  $\text{BCl}_3$  resulted in demethylation and cyclization. By contrast, the starting material was recovered largely intact following exposure to  $\text{TiCl}_4$ ,  $\text{Sc}(\text{OTf})_3$ ,  $\text{AlCl}_3$ , and  $\text{ZnCl}_2$ . Following cyclization with  $\text{BBr}_3$ , an acetylene equivalent was introduced using Sonogashira coupling to provide terminal alkyne **17**.<sup>23</sup>

Synthesis of the tetrahydroxanthone subunit started with preparation of the D-ring. Formylation of phenol **18**<sup>24</sup> was anticipated to introduce the xanthone carbonyl. However, reaction with formaldehyde under Lewis acid conditions proved unsatisfactory (Table 1, entry 1).<sup>25</sup> Phenol **18** was completely

**Table 1. Formylation and Hydroxymethylation of the D-Ring**



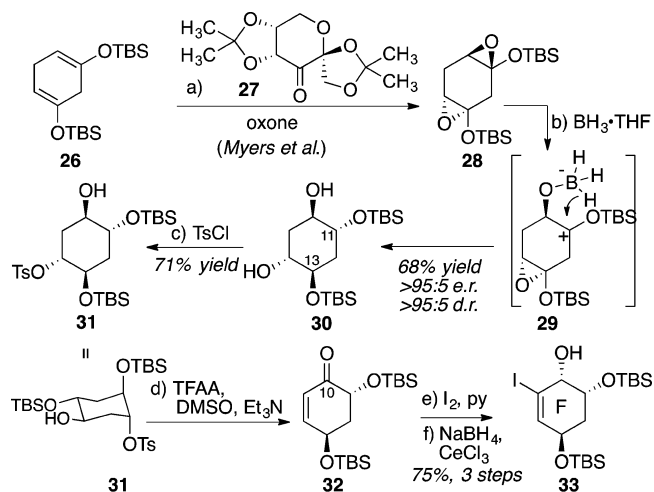
entry	R	conditions	product (Yield)
1	H	$\text{SnCl}_4$ (1 equiv), $(\text{CH}_2\text{O})_n$ , lutidine, toluene, $\Delta$	<b>20</b> (<50%)
2	H	$\text{TiCl}_4$ , $\text{MeO}-\text{CHCl}_2$	<b>20:22</b> = 1:2 (<50%)
3	H	$\text{AcOH}$ , $\text{H}_2\text{O}$ , $\Delta$ ,  ( <b>23</b> )	<b>20</b> : 40%
4	MOM	$\text{LiTMP}$ ; $\text{DMF}$ or $\text{CO}_2$	decomposition
5	H	$\text{Et}_2\text{AlCl}$ , $(\text{CH}_2\text{O})_n$ , 0 °C	<b>21</b> (91%)



consumed, and the crude reaction mixtures were remarkably clean. Nonetheless, isolated yields remained under 50% with a variety of temperature and concentration profiles. We speculate that the benzylic alcohol intermediate formed under the reaction conditions (**21**, or corresponding metal alkoxide) might have eliminated water to form the quinone methide **24**, which might have undergone polymerization. Alternative formylating agents, such as methoxydichloromethane (entry 2) or tetraazaadamantane (**23**, entry 3), provided poor regioselectivity and/or low yields.<sup>26</sup> A MOM-ether, **19**, could be cleanly lithiated, but as shown in entry 4, trapping with dimethylformamide or  $\text{CO}_2$  was not successful. Finally, we discovered that aluminum-based Lewis acids generated the benzylic alcohol **21** cleanly and in high yield (entry 5).<sup>27</sup> Subsequent protection of **21** with MOM-Cl under phase transfer conditions and oxidation gave the desired aldehyde **25** (eq 1 in Table 1).

Our synthesis of the F-ring took advantage of the pseudo- $\text{C}_2$  symmetry of the F ring that related the C11 and C13 hydroxyl groups and the C10 and C14 oxygenation. In this endeavor, we were inspired by Myers' use of the Shi epoxidation to form *trans*-diols.<sup>28,29</sup> Specifically, resorcinol was silylated and reduced with sodium in ammonia to provide the known bis-enol ether **26** (Scheme 4).<sup>28</sup> Epoxidation with the Shi catalyst (**27**) was

**Scheme 4. Enantioselective Synthesis of the F-Ring<sup>a</sup>**

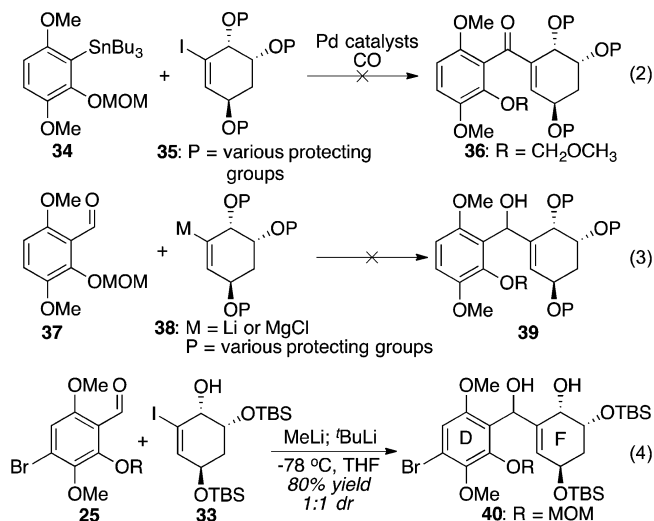


<sup>a</sup>(a) Shi catalyst (**27**, 0.6 equiv), oxone,  $\text{H}_2\text{O}$  (pH 10.5),  $\text{CH}_3\text{CN}$ , 0 °C, then (b)  $\text{BH}_3\cdot\text{THF}$ ,  $\text{Et}_3\text{O}$ , 0 °C, 68% yield over two steps, >95:5 er and dr. (c)  $\text{TsCl}$ , pyridine/ $\text{CH}_2\text{Cl}_2$  (1/1). (d) TFAA,  $\text{DMSO}$ ,  $\text{CH}_2\text{Cl}_2$ , then  $\text{Et}_3\text{N}$ , -78 °C to rt. (e)  $\text{I}_2$ , pyridine (1.2 equiv),  $\text{CH}_2\text{Cl}_2$ . (f)  $\text{NaBH}_4$ ,  $\text{CeCl}_3\cdot 7\text{H}_2\text{O}$ ,  $\text{MeOH}$ , -78 °C, 75% over three steps.

followed by immediate reduction with borane to provide the doubly protected tetraol **30** as a single observed diastereomer and enantiomer.<sup>30</sup> This reaction installed the C11 and C13 alcohols with the correct relative stereochemistry for the kibdelones. Additionally, it introduced the required oxygenation at C10 and C14. As proposed by Myers, borane presumably acts as a Lewis acid to promote ring-opening of the silyloxyoxirane (see **29**); intramolecular hydride delivery yields the protected diol. Selective monotosylation of **30** came as a welcome surprise. Analysis of  $^1\text{H}-^1\text{H}$  coupling constants for **31** suggested a *trans*-diaxial orientation of the large TBS and tosyl groups. This conformation places the remaining OH in an equatorial position, as shown. Steric hindrance from the adjacent OTBS group may prevent reaction with a second equivalent of  $\text{TsCl}$ . Next, the C10 hydroxyl was oxidized under basic conditions, which resulted in  $\beta$ -elimination of the tosyl group to yield the enone **32**. Finally, iodination and Luche reduction of the enone completed the synthesis of the F-ring iodide **33**.

With access to an appropriate F-ring vinyl iodide, we attempted to join it to the D-ring and construct the tetrahydroxanthone (Scheme 5, eqs 2–4). In preliminary studies, we were unable to effect carbonylative coupling of aryl stannane **34** with variously protected F-ring precursors (**35**, eq 2). Likewise, fully protected F-ring subunits could be metalated, but we observed no addition to the hindered and electron-rich D-ring aldehyde (eq 3). Ultimately, Li and Nicolau's synthesis of diversinol proved informative.<sup>31</sup> Thus, we speculated that the C10 protecting group might be causing steric crowding during the addition. Accordingly, we deprotonated **33** with

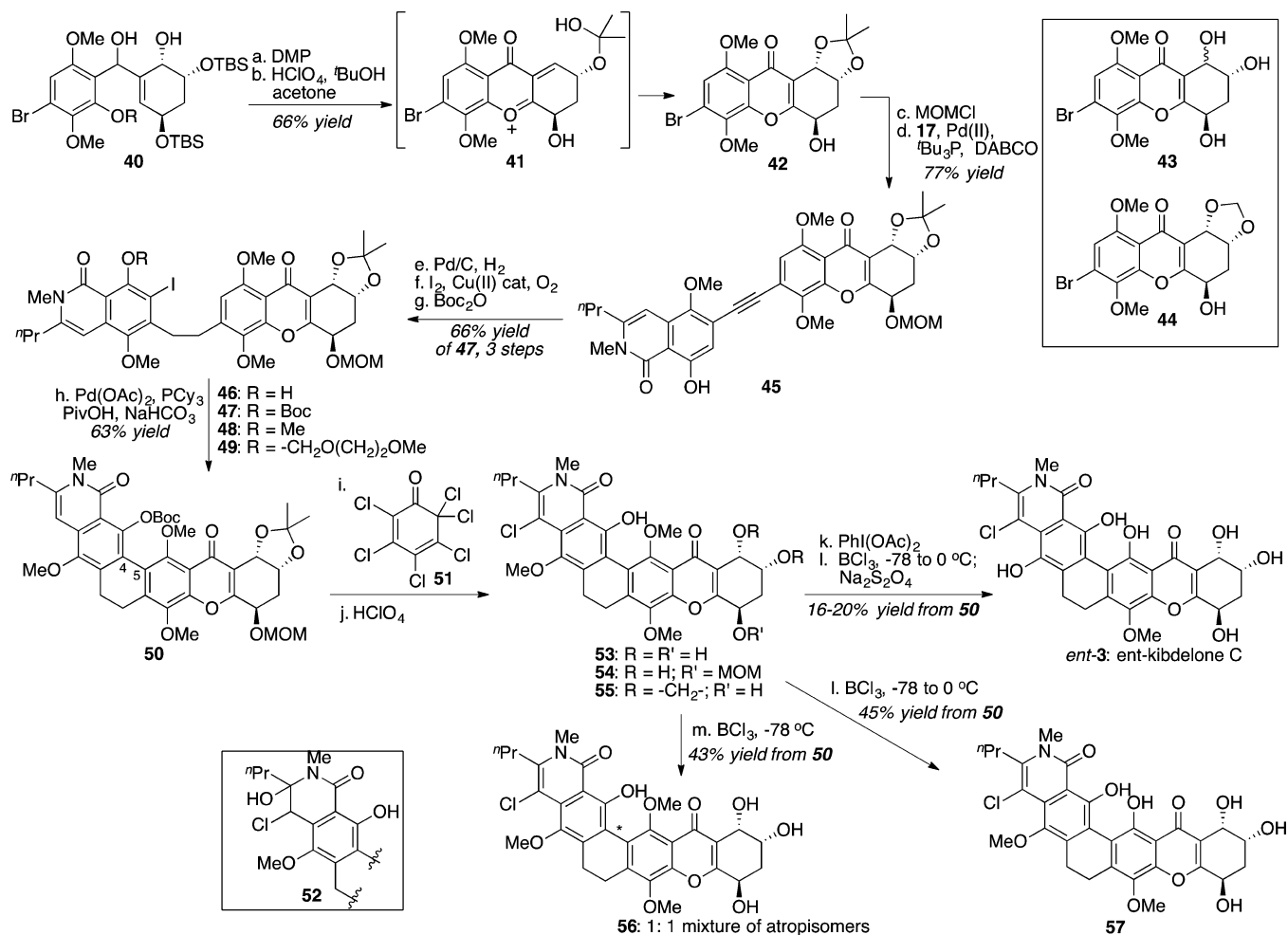
## Scheme 5. Union of the D- and F-Rings



MeLi and then converted it to the vinyl lithium with *n*-BuLi. Addition to aldehyde **25** then yielded the benzylic alcohol **40** as an inconsequential mixture of diastereomers (eq 4).

To synthesize the tetrahydroxanthone subunit, diol **40** was oxidized under Dess–Martin conditions to an unstable diketone (Scheme 6). This material was immediately exposed to perchloric acid in a mixed solvent system containing acetone and *tert*-butyl alcohol to form the tricyclic tetrahydroxanthone **42**.<sup>30</sup> This cyclization may involve intramolecular conjugate addition of acetone hemiketal **41** to install the acetonide and set the correct C10 stereochemistry. When the cyclization was performed in the absence of acetone, the triol **43** was formed as a mixture of C10 diastereomers. Likewise, when *tert*-butanol was excluded from the reaction mixture, the methylene ketal **44** was formed, presumably from the formaldehyde liberated during MOM deprotection.

**Synthesis of *ent*-Kibdelone C.** The isoquinolinone fragment was linked to the tetrahydroxanthone using a Cu-free Pd coupling.<sup>32</sup> Even in the absence of copper salts, rigorous degassing and slow addition of the alkyne were required to

Scheme 6. Synthesis of *ent*-Kibdelone C and Derivatives<sup>a</sup>

<sup>a</sup>(a) Dess–Martin periodinane, CH<sub>2</sub>Cl<sub>2</sub>. (b) HClO<sub>4</sub> (aq), <sup>t</sup>BuOH, acetone, 66% yield over two steps. (c) MOMCl, <sup>t</sup>Pr<sub>2</sub>NEt, CH<sub>2</sub>Cl<sub>2</sub>. (d) **17**, [Pd(C<sub>3</sub>H<sub>5</sub>)Cl]<sub>2</sub> (5 mol %), <sup>t</sup>Bu<sub>3</sub>P, DABCO, CH<sub>3</sub>CN/DMF 1:1, 77% yield over two steps. (e) 10% Pd/C, NaHCO<sub>3</sub> (1.5 equiv), CH<sub>2</sub>Cl<sub>2</sub>/<sup>t</sup>PrOH (1:1), H<sub>2</sub>. (f) CuCl(OH)·TMEDA (25 mol %), I<sub>2</sub>, CH<sub>2</sub>Cl<sub>2</sub>. (g) Boc<sub>2</sub>O, DMAP, CH<sub>2</sub>Cl<sub>2</sub> 66% yield over three steps. (h) Pd(OAc)<sub>2</sub> (1.5 equiv), <sup>t</sup>Bu<sub>3</sub>P·HBF<sub>4</sub> (3.0 equiv), pivalic acid (6.0 equiv), NaHCO<sub>3</sub> (20 equiv), DMA, 90 °C, 63% yield, 1:1 mixture of atropisomers. (i) **51**, DMF/CH<sub>2</sub>Cl<sub>2</sub> 5:1. (j) THF/<sup>t</sup>BuOH 2.5:1, HClO<sub>4</sub> (10 equiv). (k) PhI(OAc)<sub>2</sub> (2 equiv), CH<sub>3</sub>CN/H<sub>2</sub>O 1:1. BCl<sub>3</sub> (6 equiv), CH<sub>2</sub>Cl<sub>2</sub>, -78 to 0 °C, then Na<sub>2</sub>S<sub>2</sub>O<sub>4</sub>. (m) BCl<sub>3</sub> (6 equiv), CH<sub>2</sub>Cl<sub>2</sub>, -78 °C.



avoid oxidative coupling to form diyne side products. Hydrogenation and Cu-catalyzed iodination<sup>33</sup> yielded the phenol **46**, which could be treated with (Boc)<sub>2</sub>O to form the carbonate **47**. An intramolecular, Pd-mediated C–H arylation reaction formed the C4–C5 biaryl bond and constructed the C-ring of the natural product.<sup>34</sup> This transformation required extensive optimization, which revealed that the OBoc group, the Pd source, the temperature, and the sodium pivalate buffer were all important. The free phenol **46** or methyl ether **48** only generated trace amounts of desired product, while the (methoxyethoxy)methyl (MEM) containing substrate **49** gave around 15% of the desired product. The success of the MEM- and Boc-containing substrates indicated that these groups may coordinate to and stabilize the Pd(II) center within an aryl palladium iodide intermediate. In this cyclization, Pd(OAc)<sub>2</sub> was effective, but more Lewis acidic Pd(II) salts [e.g., PdCl<sub>2</sub>, Pd(TFA)<sub>2</sub>, Pd(OTf)<sub>2</sub>] caused aromatization of the F-ring. Likewise, at temperatures below 85 °C, only deiodination was observed, whereas at temperatures higher than 95 °C, extensive decomposition occurred. Finally, in situ generation of NaOPiv facilitated C–H functionalization, likely through a concerted metalation–deprotonation, as proposed by Fagnou and co-workers.<sup>35</sup>

Access to the full kibelone carbon skeleton allowed us to prepare the natural product and several simple derivatives. Thus, halogenation with **51** introduced the A-ring chloride, albeit with an unexpected complication. Specifically, the desired chloroisoquinolinone was accompanied by side products that we tentatively characterized as the hydration products (see **52**). Multiple stereoisomeric halohydrins were thus formed, and all of the products were generated as ~1:1 mixtures of atropisomers due to hindered rotation around the C4–C5 bond. Accordingly, no purification was possible at this stage. Next, treatment with HClO<sub>4</sub> removed the Boc group and the acetonide and prompted dehydration of the A-ring back to the isoquinolinone. However, only about half of the C13 MOM group was removed, generating similar amounts of diols **53** and **54**. Efforts to increase conversion led to decomposition. Moreover, some of the formaldehyde (or its equivalent) that formed during removal of the MOM group was trapped by the C10–C11 diol to yield the methylene ketal **55**. This mixture of products was then treated with PhI(OAc)<sub>2</sub> to remove the B-ring methyl group. Finally, exposure to BCl<sub>3</sub> cleaved the D-ring methyl group and any remaining MOM or methylene ketal. Reductive workup converted the C-ring quinone to the hydroquinone and completed the synthesis of kibelone C. The natural product was prone to oxidation, as had been reported previously. Accordingly, the final product was purified by HPLC, immediately lyophilized, and handled under an inert atmosphere.<sup>19</sup>

The specific rotation of synthetic kibelone (–40) was similar in magnitude but opposite in sign to the naturally occurring material (+47). This observation indicated that our synthetic material was enantiomeric to the natural product, a conclusion consistent with contemporaneous results from the Porco group.<sup>15b</sup>

**Synthesis and Evaluation of Initial Derivatives of Kibelone C.** We repeated the sequence shown above except for the use of the enantiomeric Shi catalyst<sup>36</sup> (*ent*-**27**) to provide the natural enantiomer for side-by-side comparison of their biological potencies (see below).<sup>22</sup> Additionally, our synthetic scheme allowed us to prepare two simple analogs to test the requirements for biological activity. In particular,

omitting the oxidative removal of the B-ring methyl group yielded methyl kibelone C (**57**). As anticipated, this compound was much more stable than the natural product, with no observed oxidative conversion to the B-ring hydroquinone under ambient conditions. Similarly, intermediate **50** was chlorinated and deprotected under acidic conditions; low-temperature treatment with BCl<sub>3</sub> retained both the B-ring and inner-rim D-ring methoxy groups to yield dimethyl kibelone C (**56**) as a 1:1 mixture of atropisomers.

The syntheses of both enantiomers of kibelone C and methyl kibelone C allowed us to answer two initial questions: Is the absolute configuration of the natural product important for biological activity, and is a quinone required for biological activity? Concerning the latter question, the Kapon group had observed rapid aerobic oxidation of kibelone C to kibelones A (**1**) and B (**2**), which feature quinone moieties. Moreover, they reported nearly identical cytotoxicity with these congeners. Since quinones are reactive to nucleophiles and can act as electron acceptors, we wondered if a quinone might be required for biological activity (eq 5). In this scenario, kibelone C would act as a pro-drug, undergoing oxidation under the assay conditions. Of relevance to this question, we noted the increased aerobic stability of methyl kibelone C, which appeared to be indefinitely stable under ambient conditions. It provided a control compound that would be less prone to generate quinones compared to the natural product. We therefore tested the cytotoxicity of both enantiomers of kibelone C and methyl kibelone C (**57**) against the colon cancer cell line HCT116. As shown in Figure 1, the four

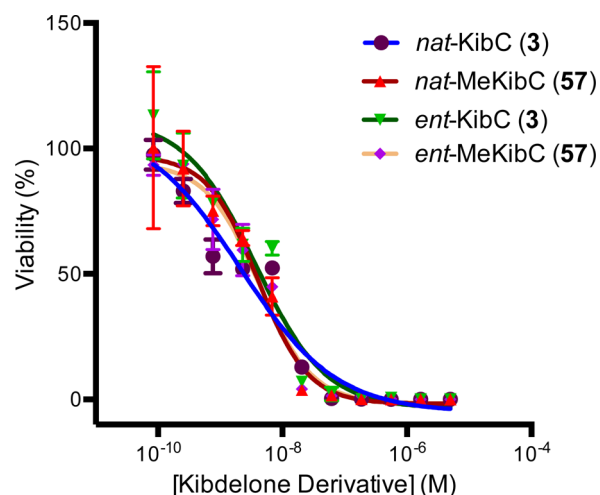
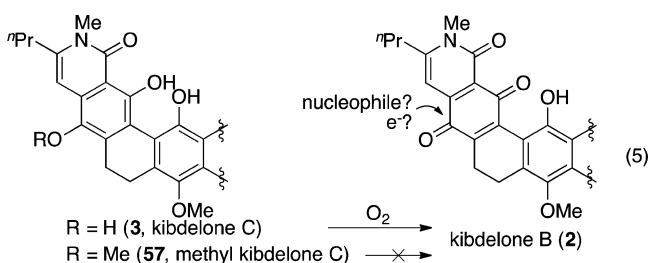


**Figure 1.** Dose–response curves of enantiomeric forms of kibelone C (**3**) and methyl kibelone C (**57**) against HCT116 colon cancer cells. Cell viability was determined with CellTiter-Glo.

compounds showed potent toxicity with overlapping dose–response curves. The concentration that resulted in 50% less viability compared to DMSO control (IC<sub>50</sub>) was calculated for each compound. The calculated IC<sub>50</sub> values were between 3 and 5 nM under these assay conditions. From these data we conclude that (a) the absolute configuration of the natural product does not affect activity, and (b) quinone formation is likely not required for biological activity.<sup>37</sup>

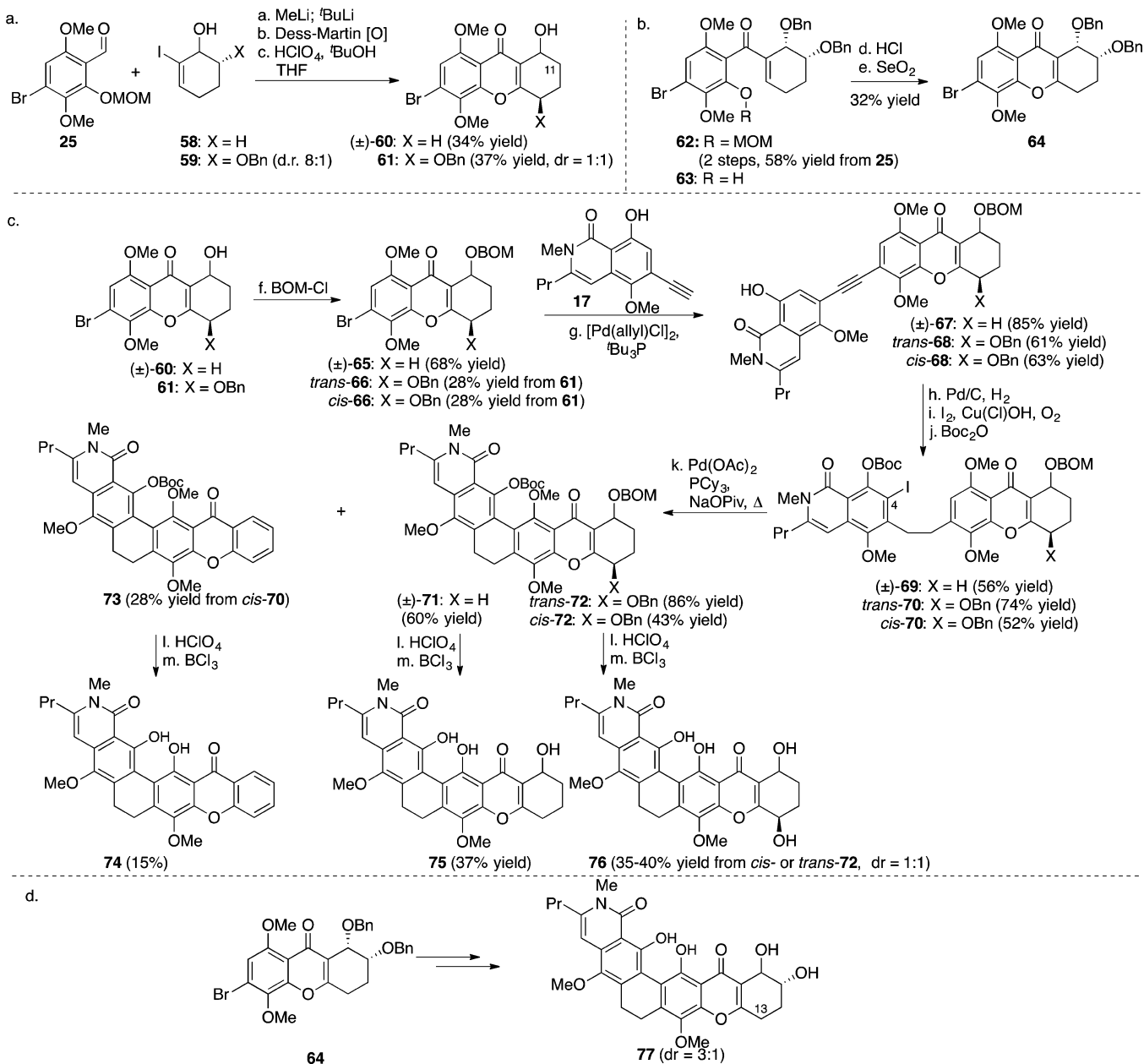
**F-Ring Derivatives of Kibelone C.** The equivalent cytotoxicity of (+)- and (–)-kibelone C is consistent with our recent discovery that the unnatural enantiomer of simaomicin  $\alpha$  shows potent cytotoxicity toward human cancer cell lines (three



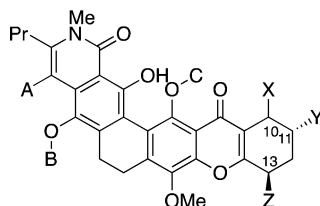
lines, IC<sub>50</sub> < 100 nM). Of note, Porco and co-workers previously found that kibelone derivatives lacking an F-ring

were >1000-fold less active than the natural product.<sup>36</sup> These observations prompted us to prepare analogs of kibelone C featuring simplified F-rings to determine the requirements for activity (Scheme 7). Toward that end, iodocyclohexenols **58** and **59** were lithiated and exposed to aldehyde **25**. Subsequent Dess–Martin oxidation and treatment with perchloric acid yielded the tetrahydroxanthones that lack oxygenation at C11 (**61**) or C11 and C13 (**60**) (Scheme 7a). As an alternative to the acid-induced cyclization, enone **62** was treated with HCl to remove the MOM group (**63**). Oxidative cyclization involving SeO<sub>2</sub> provided modest yields of the diol **64**, which lacks an alcohol at C13 (Scheme 7b).<sup>38</sup>

### Scheme 7. Synthesis of Simplified Kibelone C Derivatives<sup>a</sup>



<sup>a</sup>(a) **58** or **59**, MeLi (1.05 equiv), Et<sub>2</sub>O, then <sup>t</sup>BuLi (2.0 equiv), then **25**, THF, -78 °C. (c) HClO<sub>4</sub> (aq), <sup>t</sup>BuOH, acetone. (d) HCl, THF/H<sub>2</sub>O, rt. (e) SeO<sub>2</sub> (2.0 equiv), <sup>t</sup>BuOH, reflux. (f) Benzyloxymethyl chloride (1.5 equiv), Proton-sponge (5.0 equiv), NaI (4 equiv), THF, rt. (g) [Pd(allyl)Cl]<sub>2</sub> (5 mol %), <sup>t</sup>Bu<sub>3</sub>P·HBF<sub>4</sub> (20 mol %), DABCO (2.2 equiv), slow addition of **17**, 50 °C. (h) Pd/C, H<sub>2</sub> (1 atm), CH<sub>2</sub>Cl<sub>2</sub>/<sup>t</sup>PrOH 1:1, rt. (i) Cu(Cl)OH·TMEDA (0.25 equiv), I<sub>2</sub> (1 equiv), O<sub>2</sub> (1 atm), CH<sub>2</sub>Cl<sub>2</sub>, rt. (j) (Boc)<sub>2</sub>O, DMAP, CH<sub>2</sub>Cl<sub>2</sub>, rt. (k) Pd(OAc)<sub>2</sub> (1.5 equiv), <sup>t</sup>Bu<sub>3</sub>P·HBF<sub>4</sub> (3.0 equiv), pivalic acid (6.0 equiv), NaHCO<sub>3</sub> (20 equiv), DMA, 90 °C. (l) THF/<sup>t</sup>BuOH 2.5:1, HClO<sub>4</sub> (10 equiv). (m) BCl<sub>3</sub> (6 equiv), CH<sub>2</sub>Cl<sub>2</sub>, -78 to 0 °C.

Table 2. Cytotoxicity of Synthetic Derivatives of Kibdelone C vs Non-Small-Cell Lung Cancer Cell Lines<sup>a</sup>

compd	A	B	C	X	Y	Z	IC <sub>50</sub> (nM) of cell line		
							H157	H2073	H2122
(-)-3 <sup>b</sup>	Cl	H	H	$\beta$ -OH	OH	OH	11	23	56
(+)-3 <sup>c</sup>	Cl	H	H	$\beta$ -OH	OH	OH	11	40	79
56	Cl	CH <sub>3</sub>	CH <sub>3</sub>	$\beta$ -OH	OH	OH	3050	4760	>5000
57	Cl	CH <sub>3</sub>	H	$\beta$ -OH	OH	OH	4	11	39
74	H	CH <sub>3</sub>	H		aryl F ring		11	22	37
75	H	CH <sub>3</sub>	H	OH	H	H	11	38	39
76	H	CH <sub>3</sub>	H	OH	H	OH	1	1	4
77	H	CH <sub>3</sub>	H	OH	OH	H	2	3	5

<sup>a</sup>Cell viability measured with CellTiter-Glo. IC<sub>50</sub> values were calculated from 12-point dose–response curves in triplicate. <sup>b</sup>(-)-Kibdelone C. <sup>c</sup>(+)-Kibdelone C.

The alcohols of **60** and **61** were protected, which allowed separation of the cis and trans diastereomeric diols **66** (Scheme 7c). Separately, these aryl bromides were coupled with alkyne **17** under Cu-free conditions to yield the diaryl alkynes **67** and **68**.<sup>31</sup> Hydrogenation of the alkyne proceeded in the presence of the benzyl and BOM groups. Next, C4 was iodinated under our Cu-catalyzed conditions, and the B-ring phenol was converted to a carbonate. Iodide **69**, featuring only one alkoxy substituent on the F-ring, was cyclized in the presence of Pd(OAc)<sub>2</sub>, PCy<sub>3</sub>, and NaOPiv. This C–H arylation reaction formed the C-ring and completed the carbon skeleton to provide hexacycle **71**. Likewise, *trans*-**70** reacted cleanly under the same reaction conditions to provide the hexacyclic product *trans*-**72** in an excellent 86% yield. By contrast, the cis diastereomer, *cis*-**70**, generated the tetrahydroxanthone *cis*-**72** in only 43% yield. The reaction additionally provided the xanthone **73** containing a fully aromatic F ring. This side product arose from elimination of the benzyl and BOM ethers. Finally, removal of the benzyl, BOM, and Boc groups and the D-ring methyl of intermediates **71**–**73** gave the deprotected analogs of kibdelone C. Both the *cis*-**72** and *trans*-**72** diastereomers produced the same ~1:1 ratio of diol **76** under the acidic deprotection conditions. Using the same synthetic strategy, dibenzyl ether **64** was advanced to diol **77**, which lacks the C13 hydroxyl of kibdelone (Scheme 7d).<sup>22</sup> Of note, each of these analogs also differs from kibdelone by the absence of the A-ring chloride and the presence of the B-ring methoxy group.

Several synthetic analogs were tested for biological activity against three non-small-cell lung cancer cell lines that have been shown to display differential sensitivity to various cytotoxins.<sup>39</sup> Each cell line was treated with each compound in a 12-point dose–response experiment in triplicate ranging from 50  $\mu$ M to 30 pM. Cell viability was measured with CellTiter-Glo (Promega, Inc.) after 4 days in culture at 37 °C. The IC<sub>50</sub> values are shown in Table 2. As described above, kibdelone C and methyl kibdelone (**57**) showed low nanomolar toxicity. By contrast, dimethyl kibdelone **56**, which retains a methyl group on the convex D-ring phenol, lost >100-fold potency. Excitingly, diol **76**, which features the same F-ring as simaomicin  $\alpha$ , showed IC<sub>50</sub> values of less than 5 nM, as did

diol **77**, which lacks the C13 hydroxyl. The analog **75** retains only the C10 hydroxyl but was as active as the natural product. Finally, the simplest analog, **74**, with an unsubstituted aryl F-ring, was likewise as active as kibdelone C. Taken together, the data show that hydroxylation on the F-ring, chlorination, and a B-ring hydroquinone are not required for activity. Therefore, simplified achiral and racemic analogs maintain full cytotoxic activity, which could facilitate studies to understand their mechanism of action.

## ■ BIOLOGICAL STUDIES

**Kibdelone Does Not Bind DNA.** Molecular models of kibdelone C revealed a helical topology of the largely planar ring system. This architecture suggested the possibility that kibdelone C and its derivatives might interact with nucleic acids and/or nucleic acid-binding proteins. Indeed, polycyclic aromatic molecules can intercalate into DNA, and this activity often underpins their cytotoxicity.<sup>40</sup> To determine if intercalation into DNA was responsible for the cell killing associated with kibdelone, we attempted to rescue cells from kibdelone by adding exogenous DNA. In this experiment, the added DNA would compete with cellular DNA for binding to drug, thereby resulting in a rightward shift in the dose–response curve. As a positive control, H2122 non-small-cell lung cancer cells were treated with varying concentrations of actinomycin, an anticancer agent known to bind DNA and inhibit transcription.<sup>41</sup> In the absence of added DNA, actinomycin displayed an IC<sub>50</sub> of 0.5 nM.<sup>42</sup> However, the IC<sub>50</sub> value shifted to 51 nM in the presence of 40  $\mu$ g of herring sperm DNA (Table 3). By contrast, paclitaxel, which does not bind DNA and served as a negative control, displayed equivalent IC<sub>50</sub> values in the presence and absence of added DNA (6 nM). In the key experiment, adding exogenous DNA to the cell cultures had no impact on the toxicity of *ent*-kibdelone C. We interpret this result to indicate that kibdelone's mechanism of action does not involve binding to DNA.

**Kibdelone Does Not Inhibit Topoisomerase.** Several polycyclic, cytotoxic natural products inhibit topoisomerase, offering a potential mechanism for the toxicity observed with

**Table 3. Impact of Exogenous DNA on Cytotoxicity of Natural Products<sup>a</sup>**

compd	IC <sub>50</sub> (nM) in the presence of added DNA <sup>b</sup>			
	0 $\mu$ g	4 $\mu$ g	12 $\mu$ g	40 $\mu$ g
actinomycin	0.5	1.5	5.9	51
paclitaxel	6.4	7.8	7.2	6.4
kibdelone C	67	43	64	61

<sup>a</sup>Herring sperm DNA was added to H2122 cell cultures at the indicated levels in 96-well plates, and cells were incubated for 4 days prior to quantifying cell viability with CellTiter-Glo. <sup>b</sup>Calculated concentrations at which there were 50% fewer viable cells compared to the DMSO control.

the kibdelone family of cytotoxins.<sup>43</sup> To explore this possibility, methyl kibdelone C (**57**) was incubated with topoisomerase I and supercoiled DNA (Sc DNA). Topoisomerase I relaxes Sc DNA by introducing single-strand DNA breaks, allowing the cleaved strand to unwind, and rejoining the DNA fragments. As shown in Figure 2a, Sc DNA (lane 1) is readily relaxed to a

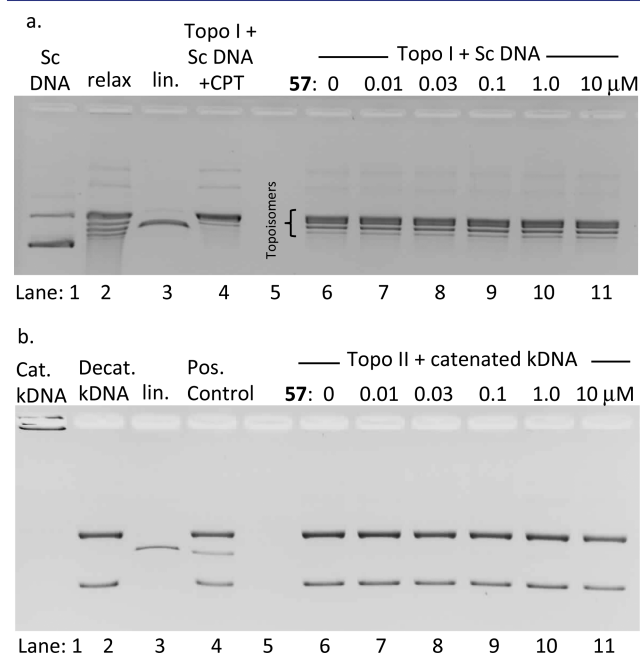


**Figure 2.** (a) Interaction of (–)-methyl kibdelone C (**57**) with topoisomerase I (Topo I). Supercoiled plasmid DNA (Sc DNA, lane 1) is converted to relaxed plasmid DNA (lane 2) by Topo I. Linear (lin.) DNA is shown for comparison (lane 3). Topo I generates nicked open circular DNA, which runs as a single band (lane 4). Methyl kibdelone does not inhibit Topo I up to 10  $\mu$ M (lanes 6–11). (b) Interaction of **57** with topoisomerase II. Catenated kinetoplast DNA (Cat. kDNA, lane 1) is converted to decatenated kDNA (lane 2) by topoisomerase II. A positive control, etoposide, induced the formation of linear DNA (lin., lanes 3, 4). Methyl kibdelone does not inhibit Topo II up to 10  $\mu$ M (lanes 6–11).

series of topoisomers in the absence of methyl kibdelone C (lane 6), and this activity is not affected by up to 10  $\mu$ M compound (lanes 7–11). While topoisomerase I induces single-strand DNA breaks, topoisomerase II creates double-strand breaks. This activity can be assayed using catenated kinetoplast DNA (kDNA), a series of interlocked circles of DNA (Figure 2b, lane 1). This high molecular weight complex can be decatenated with topoisomerase II to generate circular DNA

(lane 2). While etoposide was found to interfere with this process by generating linear DNA fragments (lanes 3, 4), methyl kibdelone C again had no effect on enzymatic activity or product distribution up to 10  $\mu$ M (lanes 6–11). We conclude that the kibdelone family of compounds does not inhibit either topoisomerase I or II.

#### Kibdelone and Derivatives Affect the Cytoskeleton.

Kibdelone C and its active derivatives caused morphological changes to human cancer cells, including cell contraction followed by cell death within 24 h. To study this activity in more detail, HeLa cells were cultured in the presence of DMSO or various cytotoxins. After 12 h, cells were fixed and stained with DAPI to mark the nuclei and with an F-actin marker (FITC–phalloidin or Alexa448–phalloidin) to observe the cytoskeleton. As shown in Figure 3A, DMSO-treated cells

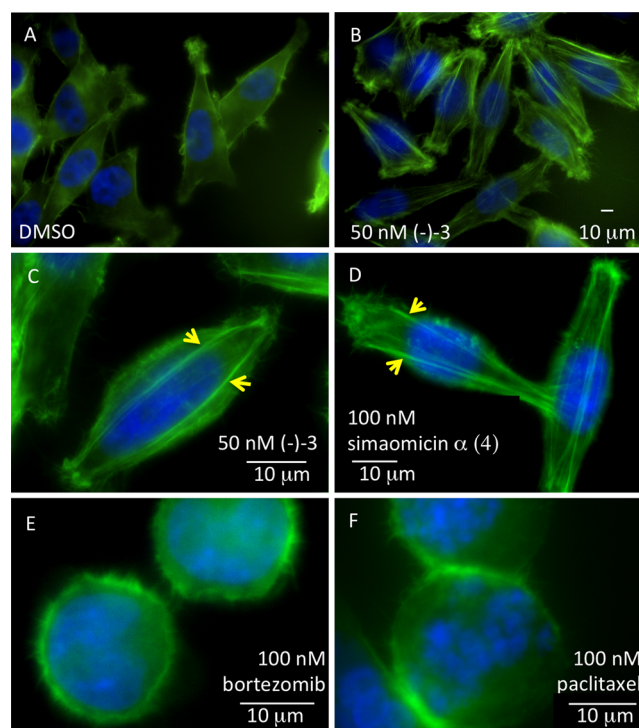


**Figure 3.** HeLa cells treated with (A) DMSO, (B and C) kibdelone C [(–)-3], (D) simaomicin  $\alpha$  (4), (E) bortezomib, or (F) paclitaxel for 12 h. Representative stress fibers are indicated with yellow arrows. Staining of nuclei (blue, DAPI) and actin (green, FITC–phalloidin) reveals cell contraction and stress fiber formation in the kibdelone- and simaomicin  $\alpha$ -treated cells.

displayed an oval-shaped nucleus and diffuse actin cytoskeleton. Cell membranes featured cortical actin structures, as expected. By contrast, *ent*-kibdelone C [(–)-3] resulted in contraction of the cells and the formation of actin fibers. Specifically, 7% of untreated cells contained these stress fibers, whereas greater than 60% of cells treated with 50 nM kibdelone C featured these structures after 12 h [Figure 3A,B; quantification in Figure S5 of the Supporting Information (SI)]. The formation of stress fibers appears to be associated with the tetrahydroxanthone family of natural products and is not a general property of cytotoxins. For example, simaomicin  $\alpha$  caused an identical phenotype (Figure 3D), as did the active analogs described above (Figure S6, SI). As shown in Figure S6 (SI), simplified analogs **57**, **76**, and **77** showed similar cell contraction/rounding and stress fiber formation as the natural



products themselves. Two representative anticancer drugs did not cause actin stress fibers to form. For example, bortezomib, a proteasome inhibitor, instead led to cell rounding without nuclear disruption. Paclitaxel, a microtubule-stabilizing agent, created disorganized nuclei and cell rounding (Figure 3E,F). This comparison indicates that the stress fibers and morphological effects are not general activities associated with cell death. Rather, they appear to be specific to the mode of action of the cytotoxic tetrahydroxanthones.

Having observed effects on the actin cytoskeleton, we considered whether kibelone C might directly affect actin polymerization. To assess this possibility, actin was polymerized in vitro in the absence or presence of kibelone C. This assay involves incorporation of tracer quantities of pyrene-labeled actin into growing actin filaments, which provides a fluorescent readout of polymerization.<sup>44</sup> Individual time-course traces are shown in Figure 4, and they demonstrate that actin

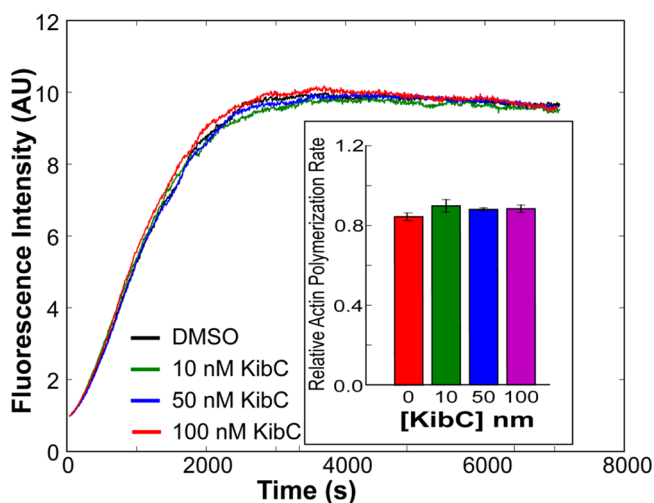


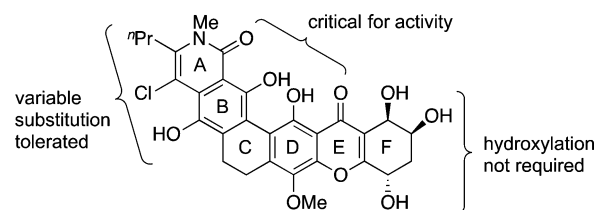
**Figure 4.** (—) Kibelone C (**3**) has no effect on the polymerization rate of actin. The main chart shows the changes in fluorescence as recombinant actin was polymerized over time ( $2 \mu\text{M}$  actin including 10% pyrene-labeled protein). Single experiments are shown in the absence or presence of the indicated concentrations of **3**. The inset shows the average rate of polymerization in the absence or presence of **3** relative to the rate in the absence of DMSO ( $n = 3$ ).

polymerization is not affected by up to 100 nM kibelone C. The inset shows the average relative rates of polymerization in the presence or absence of kibelone C ( $n = 3$ ), again indicating no effect. Taken together, the data suggests that kibelone and related compounds affect the actin cytoskeleton, but this effect does not involve a direct interaction with kibelone.<sup>45</sup>

## CONCLUSIONS

A convergent total synthesis of kibelone C allowed access to several derivatives of the natural product. Substituents around the convex periphery appear to have little impact on the biological activity. Thus, the methyl and propyl groups of the isoquinolinones of simaomicin  $\alpha$  and kibelone C both lead to potent toxicity. Similarly, the chloride of the latter natural product is dispensable. The B-ring can tolerate a cyclic ketal as in simaomicin  $\alpha$ , phenol as in kibelone C, or a methoxy group as in several synthetic derivatives. Similarly, the hydroxylation around the F-ring is apparently not required for activity (Scheme 8). Both enantiomers of kibelone C and simaomicin  $\alpha$

## Scheme 8. Structure–Activity Relationship



are active, as are analogues missing the C11 and/or C13 hydroxyls. Most surprising, an aryl F-ring lacking hydroxylation was fully active. By contrast, the hydroxyls on the concave portion of the natural product appear critical, as shown by the substantial loss in activity associated with dimethyl ether **56**. Prior studies showed that the EF-rings of the tetrahydroxanthone are indispensable.<sup>36</sup> These results suggest that the polycyclic ring system may essentially act as scaffolding to present the A- and E-ring carbonyls and B- and D-ring phenols in a defined orientation. It is perhaps noteworthy that all of the natural products shown in Scheme 1 share this functionality. This common structure could suggest a similar biological mechanism for these natural products. Moreover, it seems plausible to envision a role for metal binding by the phenols common in the B- and D-rings of the tetrahydroxanthone natural products, but that possibility remains speculative at present.

Our initial studies ruled out common modes of activity: DNA binding and topoisomerase inhibition. Cell imaging displayed profound changes to the actin cytoskeleton, but in vitro studies showed no direct effect on actin polymerization. These data indicate that the kibelones must be acting upstream of actin regulation. The structural requirements for activity and the simplified derivatives described here should facilitate the discovery of tools to identify the direct binding partners for these cytotoxins.

## ASSOCIATED CONTENT

### Supporting Information

The Supporting Information is available free of charge on the ACS Publications website at DOI: 10.1021/jacs.6b05484.

Synthetic procedures, characterization data, and supplementary figures (Figures S1–S8) (PDF)

## AUTHOR INFORMATION

### Corresponding Author

\*joseph.ready@utsouthwestern.edu

### Notes

The authors declare no competing financial interest.

## ACKNOWLEDGMENTS

Financial support came from the Welch Foundation (I-1612), CPRIT (RP101016), and the NIH (R01 GM102403). We appreciate assistance from Dr. Luke Rice with in vitro tubulin polymerization assays, from Yingli Duan with culturing cancer cells, and from Lynda Doolittle with actin polymerization assays.

## REFERENCES

- (1) Ratnayake, R.; Lacey, E.; Tennant, S.; Gill, J. H.; Capon, R. J. *Chem. - Eur. J.* **2007**, *13*, 1610–1619.

- (2) Winter, D. K.; Sloman, D. L.; Porco, J. A., Jr. *Nat. Prod. Rep.* **2013**, *30*, 382–391.
- (3) Carter, G. T.; Goodman, J. J.; Torrey, M. J.; Borders, D. B.; Gould, S. J. *J. Org. Chem.* **1989**, *54*, 4321–4323.
- (4) (a) Lee, T. M.; Carter, G. T.; Borders, D. B. *J. Chem. Soc., Chem. Commun.* **1989**, 1771–1772. (b) Maiese, W. M.; Korshalla, J.; Goodman, J.; Torrey, M. J.; Kantor, S.; Labeda, D. P.; Greenstein, M. J. *Antibiot.* **1990**, *43*, 1059–1063. (c) Koizumi, Y.; Tomoda, H.; Kumagai, A.; Zhou, X.-p.; Koyota, S.; Sugiyama, T. *Cancer Sci.* **2009**, *100*, 322–326.
- (5) Kobayashi, K.; Nishino, C.; Ohya, J.; Sato, S.; Mikawa, T.; Shiobara, Y.; Kodama, M. *J. Antibiot.* **1988**, *41*, 502–511.
- (6) Chu, M.; Truumees, I.; Mierzwa, R.; Terracciano, J.; Patel, M.; Das, P. R.; Puar, M. S.; Chan, T.-M. *Tetrahedron Lett.* **1998**, *39*, 7649–7652.
- (7) (a) Kunimoto, S.; Lu, J.; Esumi, H.; Yamazaki, Y.; Kinoshita, N.; Honma, Y.; Hamada, M.; Ohsono, M.; Ishizuka, M.; Takeuchi, T. *J. Antibiot.* **2003**, *56*, 1004–1011. (b) Kunimoto, S.; Someno, T.; Yamazaki, Y.; Lu, J.; Esumi, H.; Naganawa, H. *J. Antibiot.* **2003**, *56*, 1012–1017. (c) Lu, J.; Kunimoto, S.; Yamazaki, Y.; Kaminishi, M.; Esumi, H. *Cancer Sci.* **2004**, *95*, 547–552.
- (8) Nakagawa, A.; Omura, S.; Kushida, K.; Shimizu, H.; Lukacs, G. J. *Antibiot.* **1987**, *40*, 301–308.
- (9) Qiao, Y.-F.; Okazaki, T.; Ando, T.; Mizoue, K.; Kondo, K.; Eguchi, T.; Kakinuma, K. *J. Antibiot.* **1998**, *51*, 282–287.
- (10) Ratnayake, R.; Lacey, E.; Tennant, S.; Gill, J. H.; Capon, R. *Org. Lett.* **2006**, *8*, 5267–5270.
- (11) Kelly, T. R.; Jagoe, C. T.; Li, Q. *J. Am. Chem. Soc.* **1989**, *111*, 4522–4524.
- (12) Rao, A. V. R.; Yadav, J. S.; Reddy, K. K.; Upender, V. *Tetrahedron Lett.* **1991**, *32*, 5199–5202.
- (13) Mehta, G.; Shah, S. R.; Venkateswarlu, Y. *Tetrahedron* **1994**, *50*, 11729–11742.
- (14) Masuo, R.; Ohmori, K.; Hintermann, L.; Yoshida, S.; Suzuki, K. *Angew. Chem., Int. Ed.* **2009**, *48*, 3462–3465.
- (15) (a) Sloman, D. L.; Mitasev, B.; Scully, S. S.; Beutler, J. A.; Porco, J. A. *Angew. Chem., Int. Ed.* **2011**, *50*, 2511–2515. (b) Sloman, D. L.; Bacon, J. W.; Porco, J. A. *J. Am. Chem. Soc.* **2011**, *133*, 9952–9955.
- (16) Wang, Y.; Wang, C.; Butler, J. R.; Ready, J. M. *Angew. Chem., Int. Ed.* **2013**, *52*, 10796–10799.
- (17) (a) Yang, J.; Knueppel, D.; Cheng, B.; Mans, D.; Martin, S. F. *Org. Lett.* **2015**, *17*, 114–117. (b) Knueppel, D.; Yang, J.; Cheng, B.; Mans, D.; Martin, S. F. *Tetrahedron* **2015**, *71*, 5741–5757.
- (18) (a) Duthaler, R. O.; Heuberger, C.; Wegmann, U. H. U.; Scherrer, V. *Chimia* **1985**, *39*, 174–182. (b) Walker, E. R.; Leung, S. Y.; Barrett, A. G. M. *Tetrahedron Lett.* **2005**, *46*, 6537–6540. (c) Xiao, Z.; Cai, S.; Shi, Y.; Yang, B.; Gao, S. *Chem. Commun.* **2014**, *50*, 5254–5257.
- (19) Butler, J. R.; Wang, C.; Bian, J.; Ready, J. M. *J. Am. Chem. Soc.* **2011**, *133*, 9956–9959.
- (20) Johansson, R.; Karlstroem, S.; Kers, A.; Nordvall, G.; Rein, T.; Slivo, C. International Patent WO 039139 A1, 2008.
- (21) Barfknecht, C. F.; Nichols, D. E. *J. Med. Chem.* **1971**, *14*, 370–372.
- (22) See the Supporting Information for details.
- (23) Hundertmark, T.; Littke, A. F.; Buchwald, S. L.; Fu, G. C. *Org. Lett.* **2000**, *2*, 1729–1731.
- (24) Yonezawa, S.; Komurasaki, T.; Kawada, K.; Tsuru, T.; Fuji, M.; Kugimiya, A.; Haga, N.; Mitsumori, S.; Inagaki, M.; Nakatani, T.; Tamura, Y.; Takechi, S.; Taishi, T.; Ohtani, M. *J. Org. Chem.* **1998**, *63*, 5831–5837.
- (25) Casiraghi, G.; Casnati, G.; Puglia, G.; Sartori, G.; Terenghi, G. *J. Chem. Soc., Perkin Trans. 1* **1980**, *1*, 1862–1865.
- (26) Blazzevic, N.; Kolbah, D.; Belin, B.; Sunjic, V.; Kajfez, F. *Synthesis* **1979**, 1979, 161–176.
- (27) Bigi, F.; Casiraghi, G.; Casnati, G.; Sartori, G.; Gasparri Fava, G.; Ferrari Belicchi, M. *J. Org. Chem.* **1985**, *50*, 5018–5022.
- (28) Lim, S. M.; Hill, N.; Myers, A. G. *J. Am. Chem. Soc.* **2009**, *131*, 5763–5765.
- (29) Shi, Y. *Acc. Chem. Res.* **2004**, *37*, 488–496.
- (30) The er of tetraol **30** was determined from the bis-Mosher's ester, as described in ref 28.
- (31) Nicolaou, K. C.; Li, A. *Angew. Chem., Int. Ed.* **2008**, *47*, 6579–6582.
- (32) Soheili, A.; Albaneze-Walker, J.; Murry, J. A.; Dorner, P. G.; Hughes, D. L. *Org. Lett.* **2003**, *5*, 4191–4194.
- (33) (a) This iodination was discovered serendipitously when a sample of the reduction product of **45** containing Cu salts (from a failed attempt at Cu-promoted phenolic coupling cyclization) was exposed to *N*-iodosuccinimide. For Cu-catalyzed bromination and chlorination of arenes, see the following: Yang, L.; Lu, Z.; Stahl, S. S. *Chem. Commun.* **2009**, 6460–6462. (b) Iodination as a side reaction: Li, X.; Hewgley, J. B.; Mulrooney, C. A.; Yang, J.; Kozlowski, M. C. *J. Org. Chem.* **2003**, *68*, 5500–5511. (c) Cu(OH)Cl·TMEDA: Nakajima, M.; Miyoshi, I.; Kanayama, K.; Hashimoto, S.-i.; Noji, M.; Koga, K. *J. Org. Chem.* **1999**, *64*, 2264–2271.
- (34) Seminal contributions on C–H arylation: (a) Hennings, D. D.; Iwasa, S.; Rawal, V. H. *J. Org. Chem.* **1997**, *62*, 2–3. (b) Ackermann, L.; Vicente, R.; Kapdi, A. R. *Angew. Chem., Int. Ed.* **2009**, *48*, 9792–9826. (c) Gutekunst, W. R.; Baran, P. S. *Chem. Soc. Rev.* **2011**, *40*, 1976–1991.
- (35) Campeau, L.-C.; Parisien, M.; Jean, A.; Fagnou, K. *J. Am. Chem. Soc.* **2006**, *128*, 581–590.
- (36) Zhao, M.-X.; Shi, Y. *J. Org. Chem.* **2006**, *71*, 5377–5379.
- (37) Winter, D. K.; Endoma-Arias, M. A.; Hudlicky, T.; Beutler, J. A.; Porco, J. A. *J. Org. Chem.* **2013**, *78*, 7617–7626.
- (38) Chan, K.-F.; Zhao, Y.; Chow, L. M. C.; Chan, T. H. *Tetrahedron* **2005**, *61*, 4149–4156.
- (39) (a) For cytotoxicity screening against several NSCLC lines, including the ones used here, see data generated by the Cancer Target Discovery and Development (CTD2) Network (<https://ctd2.nci.nih.gov/dataPortal/>) established by the National Cancer Institute's Office of Cancer Genomics. (b) Theodoropoulos, P. C.; Gonzales, S. S.; Winterton, S. E.; Rodriguez-Navas, C.; McKnight, J. S.; Morlock, L. K.; Hanson, J. M.; Cross, B.; Owen, A. E.; Duan, Y.; Moreno, J. R.; Lemoff, A.; Mirzaei, H.; Posner, B. A.; Williams, N. S.; Ready, J. M.; Nijhawan, D. *Nat. Chem. Biol.* **2016**, *12*, 218–225.
- (40) (a) Prasad, K. S.; Nayak, R. *FEBS Lett.* **1976**, *71*, 171–174. (b) Shafer, R. H.; Burnette, R. R.; Mirau, P. A. *Nucleic Acids Res.* **1980**, *8*, 1121–1132. (c) Van Dyke, M.; Dervan, P. *Science* **1984**, *225*, 1122–1127.
- (41) Sobell, H. M. *Proc. Natl. Acad. Sci. U. S. A.* **1985**, *82*, 5328–5331.
- (42) Warnick-Pickle, D. J.; Byrne, K. M.; Pandey, R. C.; White, R. J. *J. Antibiot.* **1981**, *34*, 1402–1407.
- (43) (a) Latham, M. D.; King, C. K.; Gorycki, P.; Macdonald, T. L.; Ross, W. E. *Cancer Chemother. Pharmacol.* **1989**, *24*, 167–171. (b) Capranico, G.; Ferri, F.; Fogli, M. V.; Russo, A.; Lotito, L.; Baranello, L. *Biochimie* **2007**, *89*, 482–489.
- (44) Doolittle, L. K.; Rosen, M. K.; Padrick, S. B. *Methods Mol. Biol.* **2013**, *1046*, 273–293.
- (45) Kibdeleone C also does not affect the polymerization of tubulin, another common target of cytotoxic natural products. See Figure S8 (SI).